Analysis of orbital angular momentum of a misaligned optical beam

New Journal of Physics
The open–access journal for physics

Analysis of orbital angular momentum of a misaligned optical beam

M V Vasnetsov[1,3], V A Pas'ko[2] and M S Soskin[2]

[1] Optics Group, Department of Physics and Astronomy, University of Glasgow, Glasgow, UK
[2] Institute of Physics, National Academy of Sciences of Ukraine, Prospect Nauki 46, Kiev 03028, Ukraine
E-mail: m.vasnetsov@physics.gla.ac.uk

New Journal of Physics **7** (2005) 46
Received 20 July 2004
Published 9 February 2005
Online at http://www.njp.org/
doi:10.1088/1367-2630/7/1/046

Abstract. We report an analysis of the orbital angular momentum of an optical beam misaligned with respect to a reference axis. Both laterally displaced and angularly deflected Laguerre–Gaussian beams are represented in terms of the superposition of azimuthal harmonics with well-defined orbital angular momentum. Simultaneous parallel displacement and angular tilt cause the coupling between azimuthal harmonics and therefore change the projection of the orbital angular momentum on the reference axis. Rotation of beams around the reference axis was simulated by attributing corresponding rotational frequency shifts to the components.

[3] Author to whom any correspondence should be addressed.

PII: S1367-2630(05)83744-9

Contents

1. Introduction

As is well known in optics, the photon, being a quantum of electromagnetic radiation with frequency ω, possesses energy $\hbar\omega$, momentum $\hbar\omega/c$ and spin, which attains the value $\pm\hbar$ and is directed along the axis of propagation. The concept of photon orbital angular momentum (OAM) [1] has attracted much attention since Allen *et al* showed, in 1992, the possibility of separating spin and OAM contributions to the total angular momentum for paraxial light beams, namely those with helical phase structure of a wavefront [2, 3]. In contrast to the spin angular momentum, the OAM of a single photon can take any integer value in $\hbar$ units, including zero. The origin of the OAM can be explained by the orientation of a Poynting vector, possessing a nonzero azimuthal component. For instance, Laguerre–Gaussian (LG) modes LG_p^l with the azimuth index l and phase dependence in the form $\exp(\mathrm{i}l\varphi + \mathrm{i}kz)$ (where φ is the azimuthal angle and z the distance along the beam propagation) are examples of beams with helicoidal wavefronts. Geometrically, the integer l is the winding number of the wavefront helix. The light energy circulation around the beam axis produces the so-called optical vortex (OV) [4, 5]. Any OV beam with circular symmetry of intensity distribution and azimuth phase dependence $\exp(\mathrm{i}m\varphi)$ can be represented as an azimuthal harmonic with a quantized amount of the OAM per photon $m\hbar$ [2]. Hereafter, we shall refer to the winding number of a helicoid m as an orbital number.

The past decade of research efforts demonstrated the effect of OAM transfer from a light beam to small particles captured within a beam, causing their rotation [6], and the rotational Doppler effect (RDE) associated with helicoidal wavefront beams [7, 8]. The possibility of obtaining photons possessing OAM from the quantum noise [9] was shown in frequency down-conversion experiments. Expressive results of a quantum-mechanical experiment with entangled OAM states were reported recently [10]. The separation of different OAM states was shown to be possible in space, as in the frequency domain [11, 12]. The direct experimental scheme for indicating the OAM of a single photon was reported [13]. Moreover, management with photon OAM becomes possible [14].

It is natural to define OAM of a light beam with respect to its optical axis. With this choice of the reference axis, any paraxial beam can be represented as a superposition of LG modes, which are eigenmodes of the paraxial wave equation and, moreover, eigenmodes of the quantum mechanical angular momentum operator [15]. Therefore, they produce a discrete OAM spectrum, along the azimuth index of the mode (orbital number).

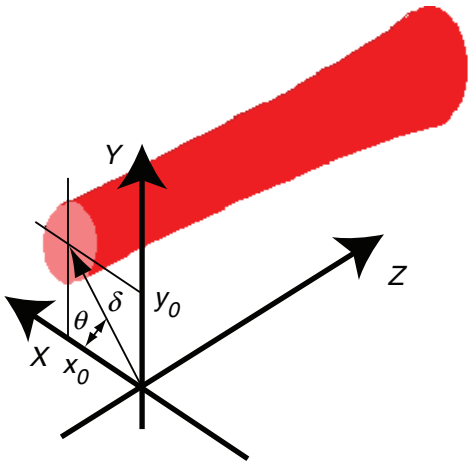

Figure 1. Schematic view of a displaced Gaussian beam. The propagation axis is parallel to the Z-axis, the radial displacement equals δ and the azimuth angle is θ.

As was shown in [16], a lateral displacement of a symmetric beam does not change its OAM. However, for an individual photon, this operation can change the photon OAM state related to the reference axis. In this sense, the pure OAM state of an individual photon in a LG mode transforms to the superposition of OAM states in a displaced coordinate frame [14]. Generally, the OAM of a light beam depends on the choice of the reference axis [14, 17] and an unambiguous determination of the reference axis for a nonsymmetric beam, e.g. a spatially truncated beam, is not possible.

The goal of the present communication is to show on an example of LG beams how a simple beam transformation generates a discrete OAM spectrum. For a lateral displacement and angular deflection, we represent the transformed beam in the form of an infinite set of azimuthal harmonics in the form of BG beams (or a more complicated structure), with a well-defined OAM. In both cases, the projection of OAM on the axis gives the intrinsic OAM of the mode, irrespective of the angle of deflection or the displacement distance. The transformation of a simultaneous shift and the tilt of a beam give quite different results. We demonstrate the coupling of OAM components, which varies the OAM projection from the intrinsic OAM of the beam.

We discuss the rotational frequency shift appearing in the azimuthal components in the case of the misaligned beam rotation around the reference axis. In order to illustrate the discrete OAM spectrum, we performed a numerical simulation of the off-axis beam rotation by attributing a corresponding frequency shift to the OAM components.

2. Lateral displacement of the LG beam

A general formula relating the decomposition of an optical beam into a set of azimuthal harmonics with respect to the arbitrary reference axis is given in [14]. Below we will show practical results for displaced Gaussian and LG beams.

Let us consider a Gaussian beam with amplitude E_0 and waist transversal dimension w_0, so the amplitude distribution in the waist attains the form $\sim E_0 \exp[-(x^2 + y^2)/w_0^2]$. In the coordinate frame (figure 1), which is laterally displaced with respect to the optical axis of the beam,

the parallel displacement is determined by the values x_0 and y_0. Therefore, at $z = 0$, the displaced Gaussian beam can be written as

$$E_S(x, y) = E_0 \exp\left(-\frac{(x - x_0)^2 + (y - y_0)^2}{w_0^2}\right). \tag{1}$$

In polar coordinates, by letting $x_0 = \delta\cos\theta$ and $y_0 = \delta\sin\theta$ (as shown in figure 1), we obtain

$$E_S(\rho, \varphi) = E_0 \exp\left(-\frac{\rho^2 + \delta^2}{w_0^2}\right) \exp\left(\frac{2\rho\delta\cos(\varphi - \theta)}{w_0^2}\right). \tag{2}$$

This form can be represented through the decomposition of the second exponent as

$$E_S(\rho, \varphi) = E_0 \exp\left(-\frac{\rho^2 + \delta^2}{w_0^2}\right) \sum_{m=-\infty}^{\infty} I_m\left(\frac{2\rho\delta}{w_0^2}\right) \exp[\mathrm{i}m(\varphi - \theta)], \tag{3}$$

where I_m is the modified Bessel function of integer order m [18]. In this way, we come to an infinite set of BG beams [19] with the azimuth phase dependence $\exp(\mathrm{i}m\varphi)$. As a result of these transformations, the laterally displaced Gaussian beam appears as a superposition of axial BG beams. Each BG component possesses the corresponding orbital number m.

The use of the BG basis is an alternative to the LG-mode basis, and they can be easily transformed into each other, if necessary. The result of a superposition of the BG beams is shown in figure 2. A single zero-order BG component looks like an axial beam (figure 2(a)), while the superposition of the zero-order BG beam and plus/minus first-order beams definitely produces an off-axis spot (figure 2(b)). The result of a superposition of 11 components, from $m = -5$ to 5, is shown in figure 2(c), with high accuracy restores the displaced Gaussian beam.

Each BG component represents an azimuthal harmonic with the orbital number m and therefore $m\hbar$ OAM per photon [2]. The circular symmetry of the intensity distribution ensures the pure OAM state of a photon belonging to each component. Figure 3 shows the calculated power spectrum of the OAM components (part of the total beam power carrying with the component) for the case of the displacement δ equal to the waist parameter w_0 of the Gaussian envelope. As is seen, the power of the components with the numbers $|m| > 3$ is negligible (figure 3(a)). Larger displacement broadens the spectrum, as shown in figure 3(b). The calculated dispersion of the spectrum was found to be proportional to the displacement, in the form $\left(\sum_{-\infty}^{\infty} m^2 P_m\right)^{1/2} = \delta/w_0$, where P_m are normalized power weights of the m components.

The same operation can be applied for the high-order LG mode with amplitude parameter E_{LG}. Let us consider a mode LG_0^l at the waist $z = 0$, which is shifted parallel to the Z-axis:

$$E_S(x, y) = E_{LG}\left[\frac{(x - x_0) + \mathrm{i}(y - y_0)}{w_0}\right]^l \exp\left[-\frac{(x - x_0)^2 + (y - y_0)^2}{w_0^2}\right]. \tag{4}$$

In cylindrical coordinates, we get, by decomposition of the Gaussian term into a set of BG components,

$$E_S(\rho, \varphi) = \frac{E_{LG}}{w_0^l}(\rho e^{\mathrm{i}\varphi} - \delta e^{\mathrm{i}\theta})^l \exp\left(-\frac{\rho^2 + \delta^2}{w_0^2}\right) \sum_{m=-\infty}^{\infty} I_m\left(\frac{2\rho\delta}{w_0^2}\right) \exp[\mathrm{i}m\,(\varphi - \theta)]. \tag{5}$$

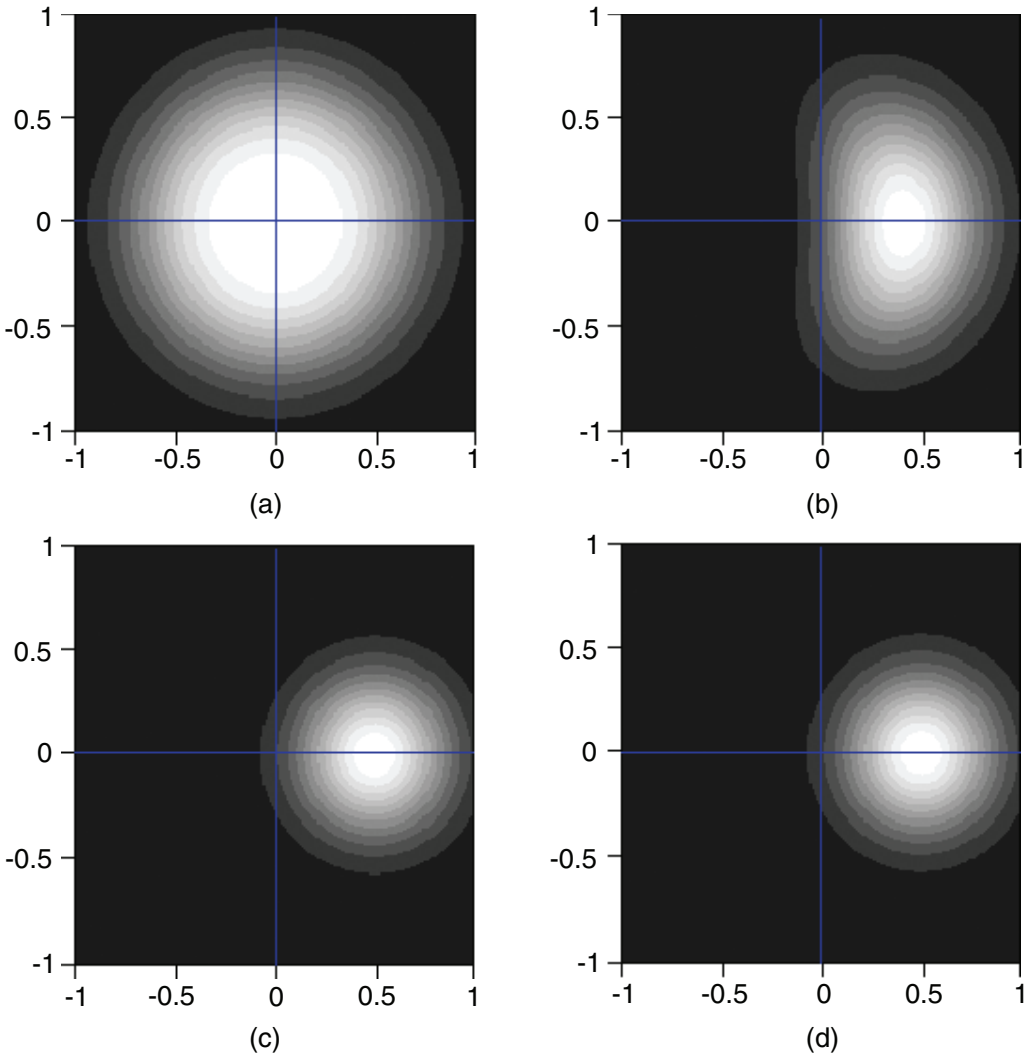

Figure 2. Construction of the displaced Gaussian beam from axial BG beams: (a) the zero-order BG component alone, (b) superposition of the zero-order BG beam and plus/minus first-order BG beams, (c) a result of the superposition of 11 BG components from $m = -5$ to 5 and (d) the Gaussian displaced beam.

Using the binomial decomposition, we come to the result for the displaced beam

$$E_S(\rho, \varphi) = \sum_{m=-\infty}^{\infty} A_{ml}(\rho, \delta) \exp[\mathrm{i}m\varphi - \mathrm{i}(m-l)\theta], \tag{6}$$

where

$$A_{ml}(\rho, \delta) = \frac{E_{LG}}{w_0^l} \exp\left(-\frac{\rho^2 + \delta^2}{w_0^2}\right) \sum_{n=0}^{l} C_l^n \rho^n (-\delta)^{l-n} I_{m-n}\left(\frac{2\rho\delta}{w_0^2}\right) \tag{7}$$

are amplitudes of the OAM components, and C_l^n are binomial coefficients. The obtained OAM spectrum is symmetric with respect to $m = l$. This ensures that the total OAM, as an arithmetic

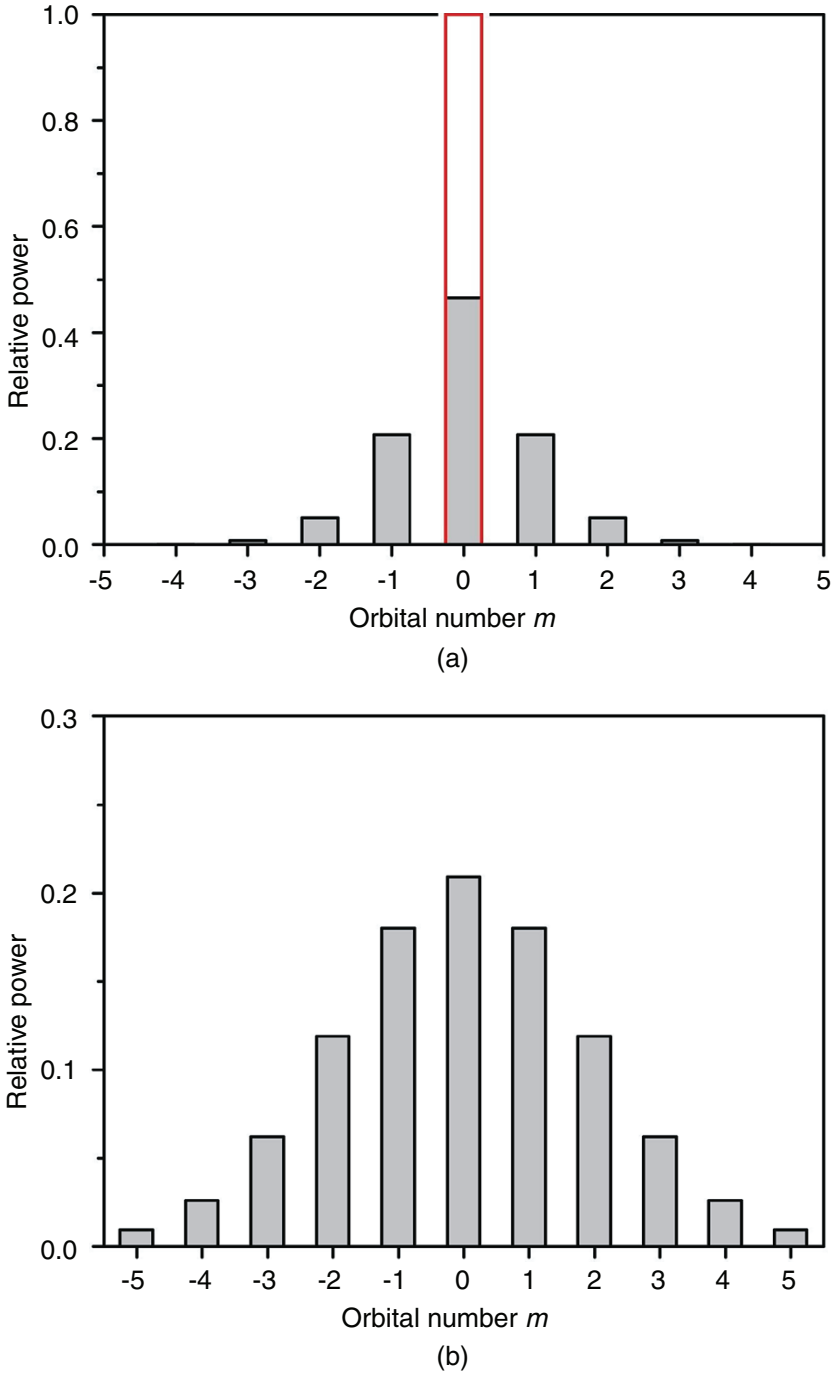

Figure 3. Power spectrum of the OAM components versus the orbital number m. The height of a peak shows the relative weight for the corresponding BG component. The red empty box shows the intrinsic OAM power spectrum of the non-displaced beam. (a) Spectrum for a Gaussian beam displaced on a distance $\delta = w_0$. (b) The spectrum for larger displacement $\delta = 2w_0$.

sum of the contribution of all components, is the same as that for the initial (nondisplaced) beam. The same is valid, of course, for a Gaussian beam ($l = 0$).

As an example, the OAM power spectrum is shown in figure 4 for a displaced LG_0^1 mode, for two displacement values. In contrast to the Gaussian beam, the broadening of the spectrum is accompanied by a depletion of the central component (figure 4(b)).

3. Angular deflection of a beam

In a similar way, we can consider a Gaussian beam propagating at some angle γ to the reference axis, as shown in figure 5. The angular deviation of a beam from its initial direction of propagation also results in the appearance of discrete OAM components. Below, we shall restrict ourselves to a range of moderate angles of deflection. The restriction on the deflection angles follows from the structure of a paraxial BG beam description, which assumes that the transversal component of a wavevector k_ρ is significantly smaller than the longitudinal one, i.e. $k_\rho^2 \ll k_z^2$, and therefore

$$k_z = \left(k^2 - k_\rho^2\right)^{1/2} \approx k - k_\rho^2/2k. \tag{8}$$

Within this limitation, we can represent a deflected Gaussian beam as the beam passing through a phase wedge with the transmission function $\exp[\mathrm{i}\alpha\rho\cos(\varphi - \eta)]$, where α is related to the deflection angle γ, $\alpha = k_\rho = k\sin\gamma$ and η is the azimuth angle of the deflection. Then, we can rewrite the transmission function by a decomposition in terms of the Bessel functions and obtain a description of the deflected beam:

$$E_T(\rho, \varphi) = E_0 \exp\left(-\frac{\rho^2}{w_0^2}\right) \sum_{m=-\infty}^{\infty} J_m(\alpha\rho) \exp\left[\mathrm{i}m\left(\varphi - \eta + \frac{\pi}{2}\right)\right]. \tag{9}$$

The obtained decomposition of the deflected Gaussian beam to the set of BG beams possesses the symmetric OAM spectrum, shown in figure 6 for the deflection angle $\gamma = 2.5 \times 10^{-4}$ (the parameter $\alpha = 2.5\,\mathrm{mm}^{-1}$).

Free space propagation of the beam will be described as the interference of these components taking into account their Gouy phase shifts [20]. The equation for free space propagation of a BG beam of the order m has the form

$$E_{BG}(\rho, z) = E_{BG}\frac{w_0}{w}\exp\left[\left(-\frac{1}{w^2} + \frac{\mathrm{i}k}{2R(z)}\right)\left(\rho^2 + \frac{\alpha^2 z^2}{k^2}\right)\right] J_m\left(\frac{\alpha\rho}{1 + \mathrm{i}z/z_R}\right)$$
$$\times \exp\left\{\mathrm{i}\left[\left(k - \frac{\alpha^2}{2k}\right)z - \Phi(z) + m\varphi\right]\right\}, \tag{10}$$

where z_R is the Rayleigh range, $\Phi(z)$ is the Gouy phase shift and $R(z)$ is the wavefront spherical curvature attributed to the Gaussian envelope of the beam: $\Phi(z) = \arctan(z/z_R)$, $R(z) = z + z_R^2/z$.

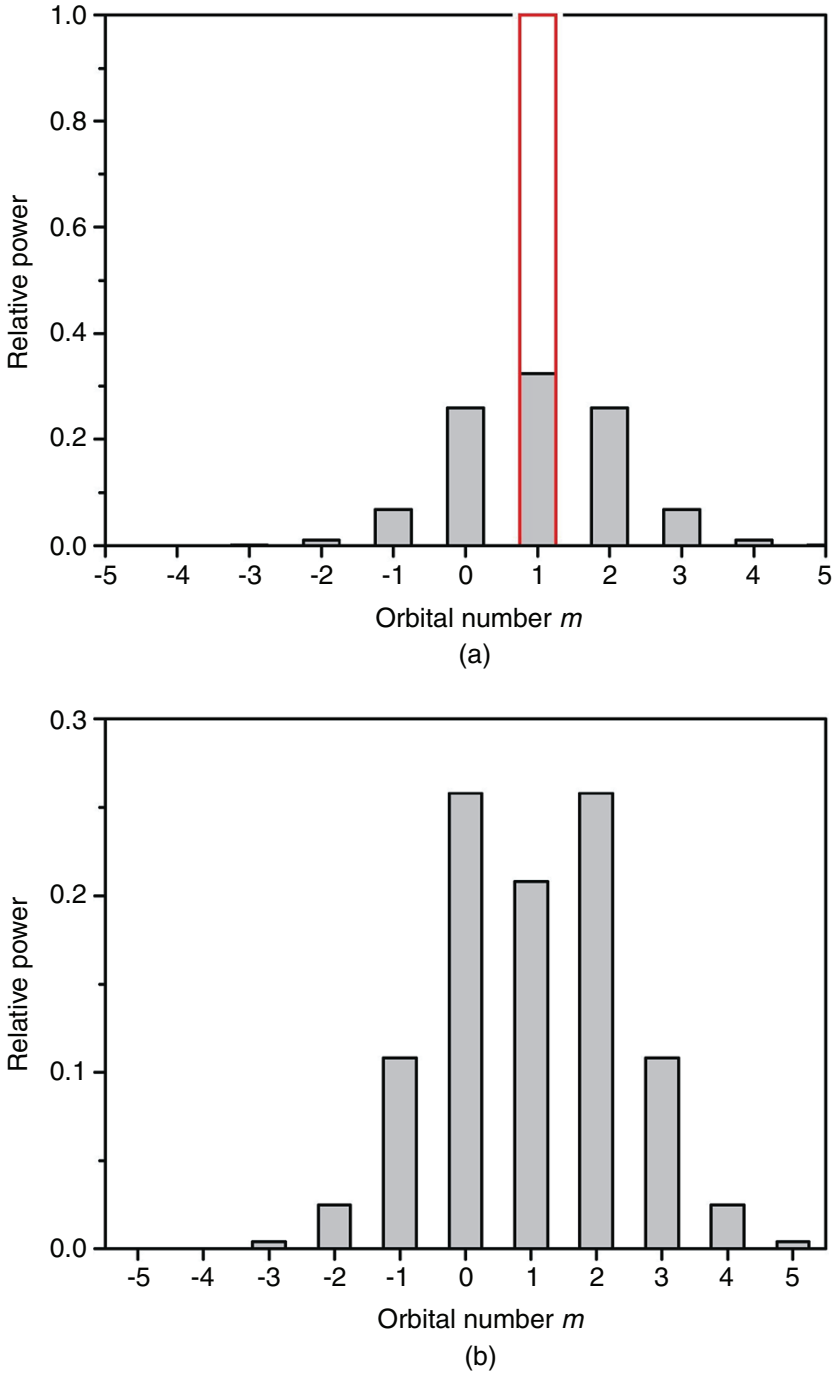

Figure 4. (a) Power spectrum of the OAM components for the parallel displacement of a LG_0^1 mode by a distance $\delta = 0.8w_0$. The red open box shows the intrinsic OAM power spectrum of the nonperturbed beam. (b) The same spectrum for a displacement $\delta = w_0$.

With these axial BG beams, we can construct the deflected beam via superposition (9) at any distance from the deflection element.

The analysis of the OAM spectrum of a deflected beam, carrying initially non-zero OAM in a pure state $l\hbar$ per photon (e.g. LG LG_0^l mode), is also straightforward. With the use of the

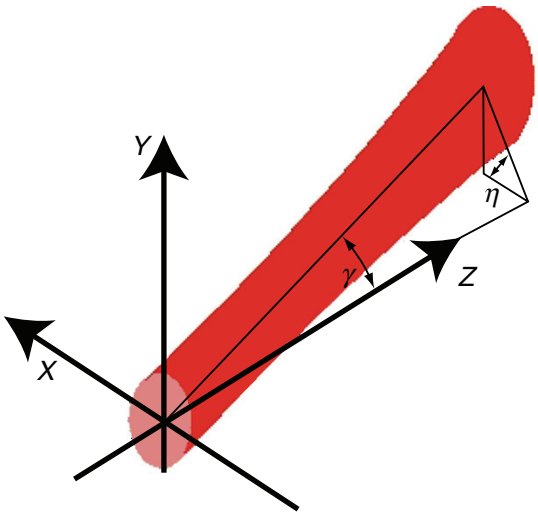

Figure 5. Schematic view of a deflected Gaussian beam. The angle of deflection is γ and the azimuth angle is η.

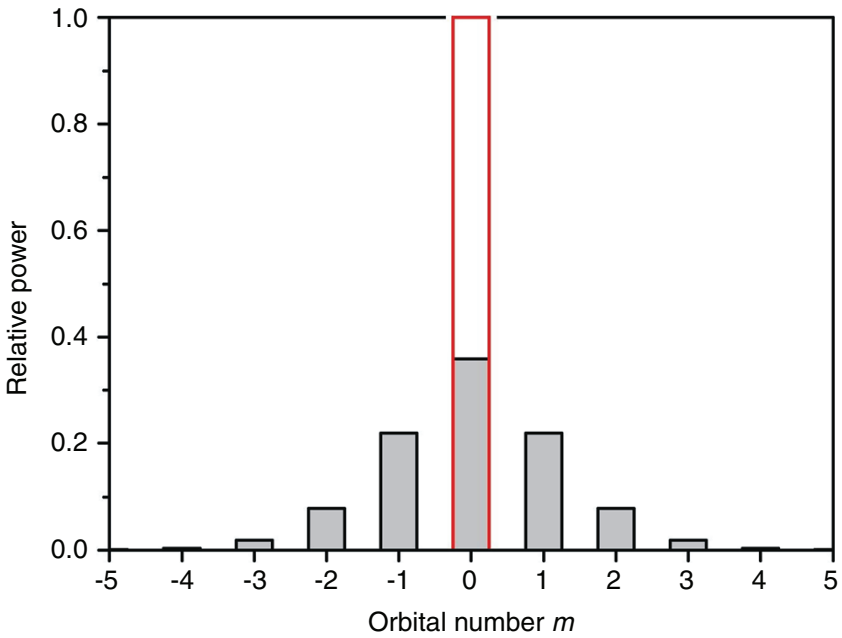

Figure 6. Power spectrum of the OAM components in the deflected Gaussian beam for the angle of deflection $\gamma = 2.5 \times 10^{-4}$.

phase wedge function decomposition (9), we get

$$E_T(\rho, \varphi) = \frac{E_{LG}}{w_0^l} \rho^l \mathrm{e}^{\mathrm{i}l\varphi} \exp\left(-\frac{\rho^2}{w_0^2}\right) \sum_{m=-\infty}^{\infty} J_m(\alpha\rho) \exp\left[\mathrm{i}m\left(\varphi - \eta + \frac{\pi}{2}\right)\right] \tag{11}$$

or

$$E_T(\rho, \varphi) = \sum_{m=-\infty}^{\infty} B_{ml}(\rho) \exp[\mathrm{i}m\varphi - \mathrm{i}(m-l)\eta]. \tag{12}$$

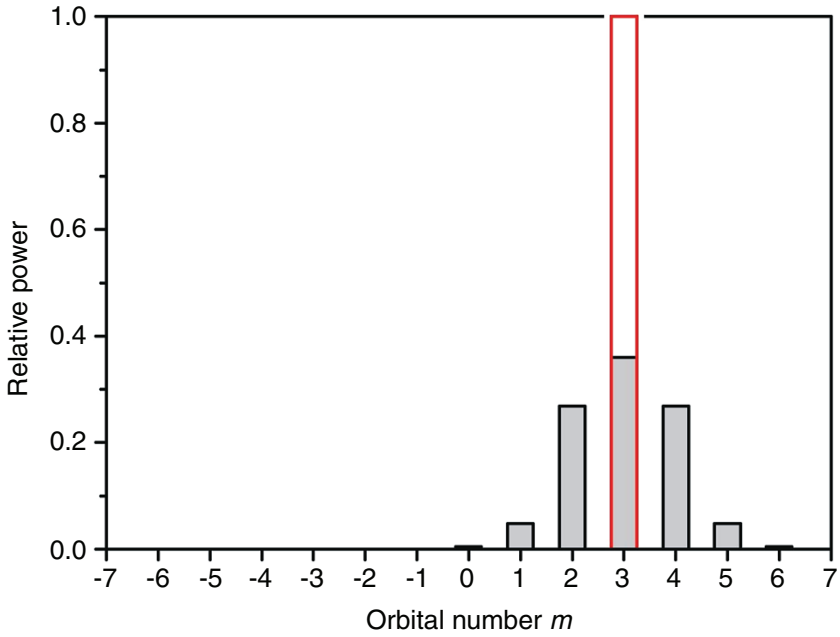

Figure 7. Power spectrum of OAM components of a deflected LG_0^3 beam. The spectrum is symmetric around the component with the orbital number $m = l = 3$.

The complex amplitude of an OAM spectral component B_{ml} is

$$B_{ml}(\rho) = \frac{E_{LG}}{w_0^l}\rho^l J_{m-l}(\alpha\rho)\exp\left(-\frac{\rho^2}{w_0^2}\right)\exp\left[\mathrm{i}(m-l)\frac{\pi}{2}\right]. \tag{13}$$

These amplitude distributions do not correspond to a solution of the wave equation, and therefore it will be necessary to represent them through a set of LG modes for a description of their free space propagation. However, the phase dependence in equation (12) ensures a pure OAM state in each component. Figure 7 shows the corresponding spectrum for a deflected LG_0^3 beam with the deflection angle $\gamma = 2.5 \times 10^{-4}$.

Some important conclusions can be obtained immediately: the OAM spectrum is symmetric around $m = l$. Another consequence is that the total angular momentum carried by the OAM components is exactly the same as that for the initial beam. In this sense, the projection of the OAM of the deflected beam does not coincide with a geometrical projection, which depends on the angle γ.

4. Combination of the tilt and lateral displacement

In any practical situation, a light beam can experience both tilt and displacement (figure 8) with respect to the reference axis. The transformation of an LG mode, which experiences a

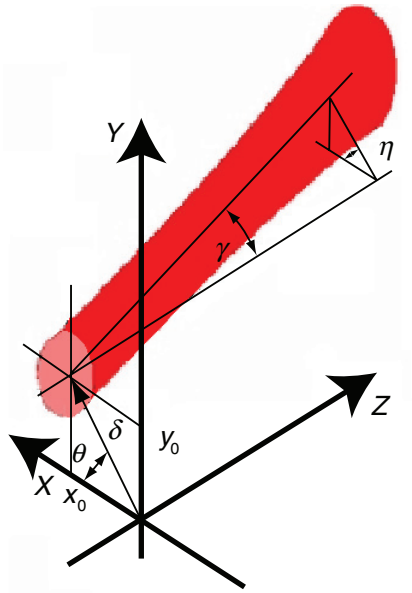

Figure 8. Schematic view of the simultaneously tilted and shifted Gaussian beam.

misalignment simultaneously by shift and tilt, is of the form

$$E(\rho,\varphi) = \frac{E_{LG}}{w_0^l}(\rho e^{i\varphi} - \delta e^{i\theta})^l \exp\left(-\frac{\rho^2+\delta^2}{w_0^2}\right) \sum_{m=-\infty}^{\infty} I_m\left(\frac{2\rho\delta}{w_0^2}\right) \times \sum_{n=-\infty}^{\infty} J_n(\alpha\rho) \exp\left[im(\varphi-\theta) + in\left(\varphi-\eta+\frac{\pi}{2}\right)\right] \tag{14}$$

(here δ is the displacement, α the tilt parameter and θ and η are azimuth angles of shift and tilt, respectively).

After mathematical operations, similar to that used above, we get

$$E_{ST}(\rho,\varphi) = \sum_{m=-\infty}^{\infty} C_{ml}(\rho) \exp[im\varphi - i(m-l)\theta]\,. \tag{15}$$

The complex amplitude of an OAM spectral component $C_{ml}(\rho)$ is

$$C_{ml}(\rho) = \frac{E_{LG}}{w_0^l} \exp\left(-\frac{\rho^2+\delta^2}{w_0^2}\right) \sum_{n=0}^{l} C_l^n \rho^n (-\delta)^{l-n} S_{m-n}, \tag{16}$$

where

$$S_m = \sum_{n=-\infty}^{\infty} I_{m-n}\left(\frac{2\rho\delta}{w_0^2}\right) J_n(\alpha\rho) \exp\left[in\left(\theta-\eta+\frac{\pi}{2}\right)\right]. \tag{17}$$

The resulting OAM spectrum will no longer be symmetric, except for special combinations of angles θ and η. It is evident that even a Gaussian beam may achieve nonzero OAM with respect to the reference axis. The skew beam attains an extrinsic OAM, due to

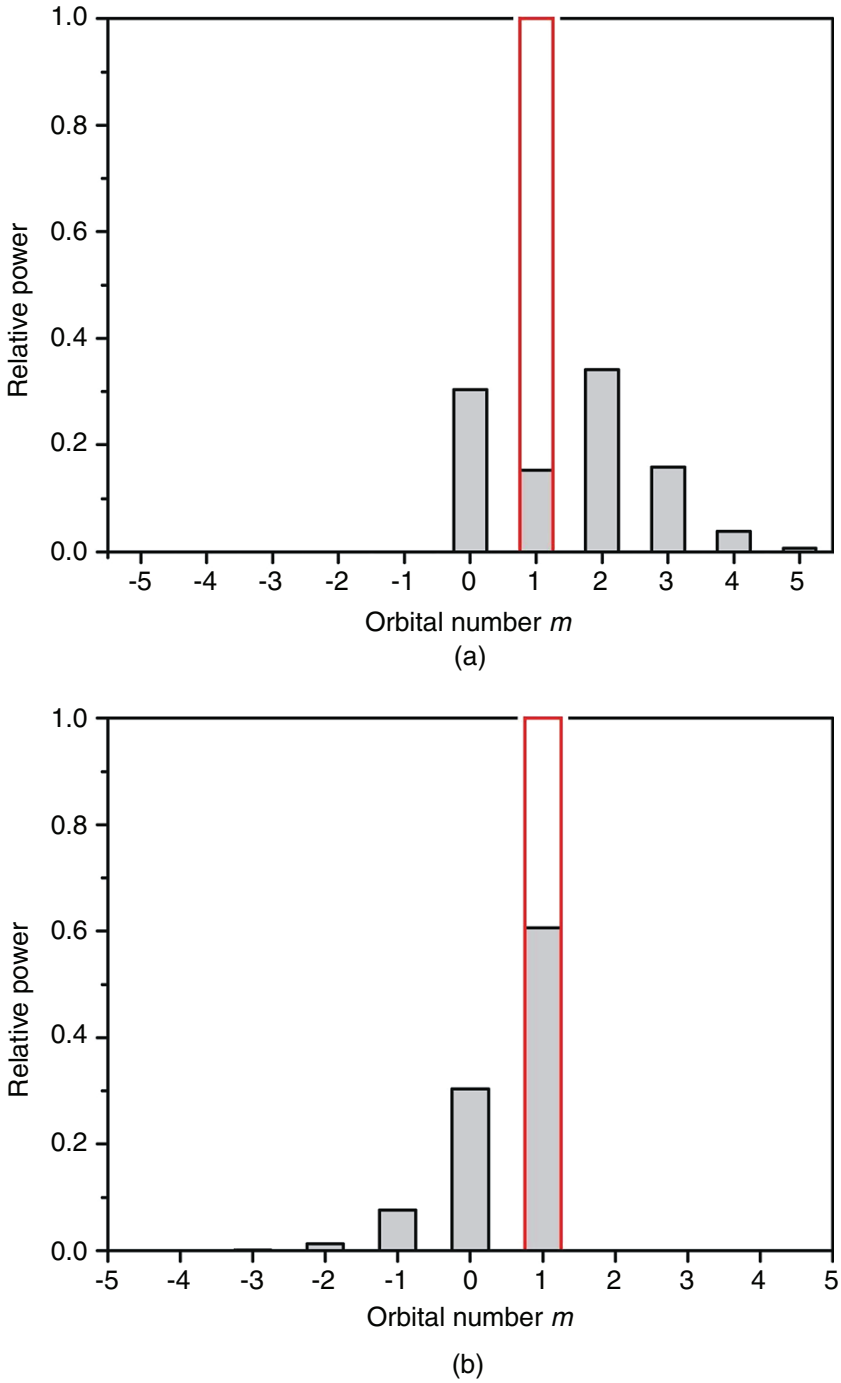

Figure 9. OAM power spectrum of LG_0^1 mode, which is displaced by a distance $\delta = 0.5w_0$ to the origin and tilted by an angle $\gamma = 10^{-4}$. (a) Azimuth parameters are $\theta = 0$, $\eta = \pi/2$; (b) $\theta = \pi/2$, $\eta = 0$.

the appearance of a transversal linear momentum. The total OAM projection will be a superposition of the intrinsic and extrinsic ones. Moreover, the contribution of the extrinsic OAM depends on both the angles θ and η, and therefore beam rotation around the reference axis will vary the OAM projection to the axis. Figure 9 shows OAM spectra for two cases,

opposite in the sense of the contributions of an extrinsic OAM and the intrinsic one to the total OAM.

5. Off-axis beam rotation and RDE

To resolve the OAM spectrum experimentally, one can use the so-called rotational frequency shift or RDE, which appears for rotating beams, bearing nonzero OAM [6, 7, 11]. High-frequency rotation of a displaced or tilted LG beam around the reference axis will generate sidebands around its optical frequency with the frequency separation equal to the frequency of the beam rotation. However, to detect the sidebands, for instance with a Fabry-Perot interferometer, extremely high angular velocities are required [11]. At the moment, the direct experiment looks rather complicated, but we can perform a reciprocal operation by computer simulation. Each OAM component in equation (3) is supposed to attain a corresponding frequency shift $m\Omega$, along the transformation $\theta = \Omega t$, which results in the rotation of the light spot as a whole with the angular velocity Ω. Moreover, it is not necessary to use the whole infinite spectrum to get the proper rotation, as higher BG components do not influence the angular velocity of the spot rotation. The animation shows the off-axis beam rotation.

Continuous rotation of the displaced LG mode around the Z-axis, expressed mathematically as $\theta = \Omega t$, generates a frequency shift equal to $(m - l)\Omega$ for the m component. The conclusion is that the only difference between input and output photon OAM state can generate a frequency shift in the OAM component by a rotating element. Another important conclusion is that the RDE spectrum is symmetric around the zero-frequency shift in this case, independent of l. The reason is that the central component in the OAM spectrum with orbital number $m = l$ attains no frequency shift, while the component with $m = l + n$ attains $n\Omega$ shift for any integer n.

Figure 10 shows the RDE spectra, which correspond to the OAM spectra of displaced Gaussian and LG beams, shown in figures 3 and 4. Initially, the monochromatic beam becomes polychromatic, with sidebands around the optical frequency of the beam. The amplitude of the sidebands depends on the beam displacement, while the frequency separation equals the frequency of the beam rotation. The beam rotation will not change the total beam energy, since the influences of positive and negative RDE frequency shifts will balance each other. Therefore, we can expect zero phase variation in rotating the displaced LG beam. (We note, however, that this result is valid only for the initially pure OAM state of the beam.)

In the case of a tilted Gaussian or LG beam, the corresponding RDE spectrum is also symmetric around zero-frequency shift, as figure 11 shows for the LG_0^3 mode. The origin of the frequency shift is easily understandable from equation (12), since the rotation of the deflection element produces azimuthal angle variation $\eta = \Omega t$, thus generating the frequency shift $(m - l)\Omega$ for the m component. In a computer simulation, this frequency shift can be attributed to the OAM components to simulate the rotation of the beam.

As a consequence, the rotation of the deflected beam around the Z-axis will not change the beam energy and will not influence the phase of the beam. The same is valid, of course, for a Gaussian beam ($l = 0$).

A combination of the shift and tilt of the beam radically changes the situation. The OAM projection to the reference axis is no longer equal to the intrinsic OAM of

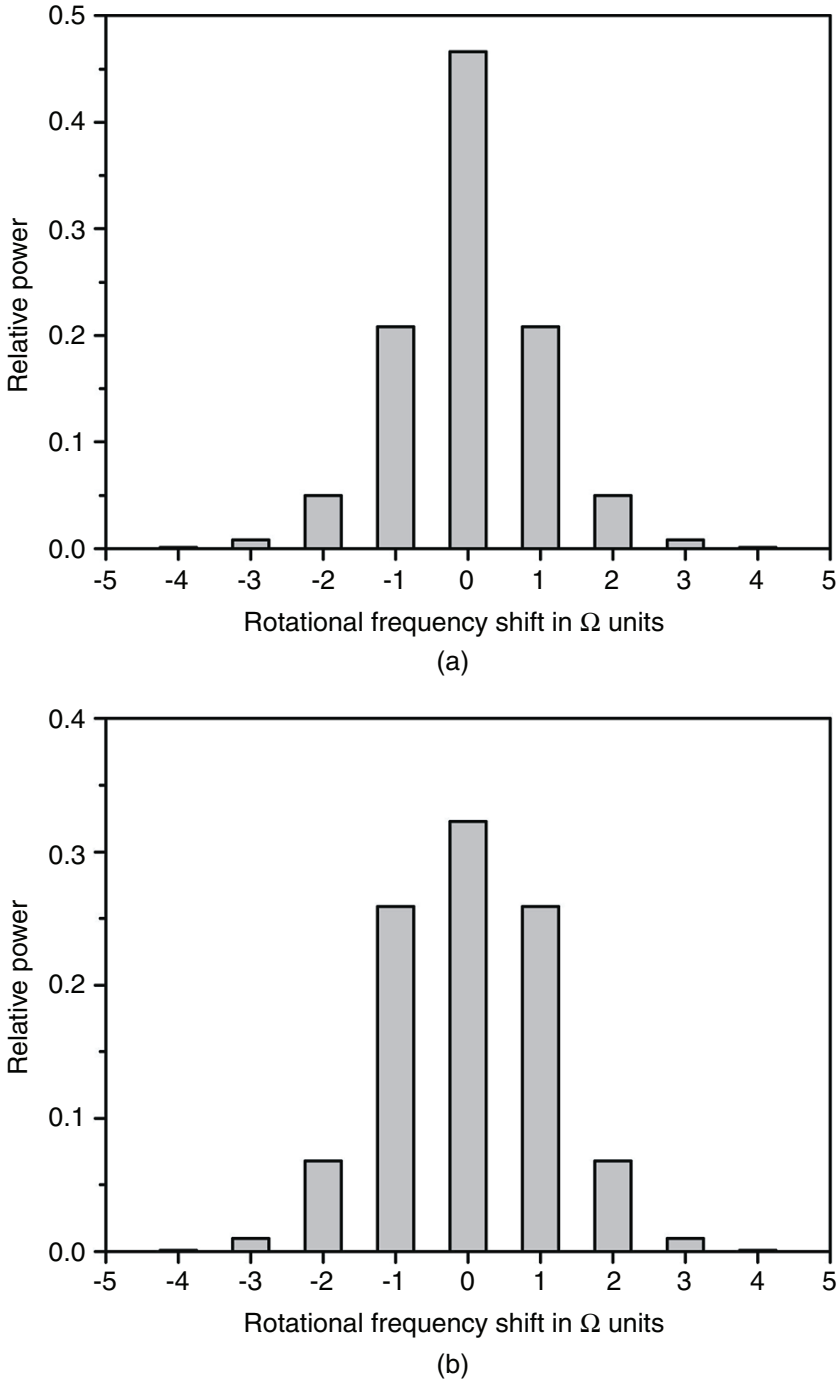

Figure 10. (a) RDE spectrum of a displaced Gaussian beam rotating with frequency Ω around the reference axis, in Ω units, on the horizontal axis. (b) The same spectrum for the LG_0^1 mode. The displacements of beams are w_0 (a) and $0.8w_0$ (b).

the beam and depends on the beam orientation. Rotation of the beam causes variation of the OAM projection on the axis, and the RDE spectrum becomes rather complicated.

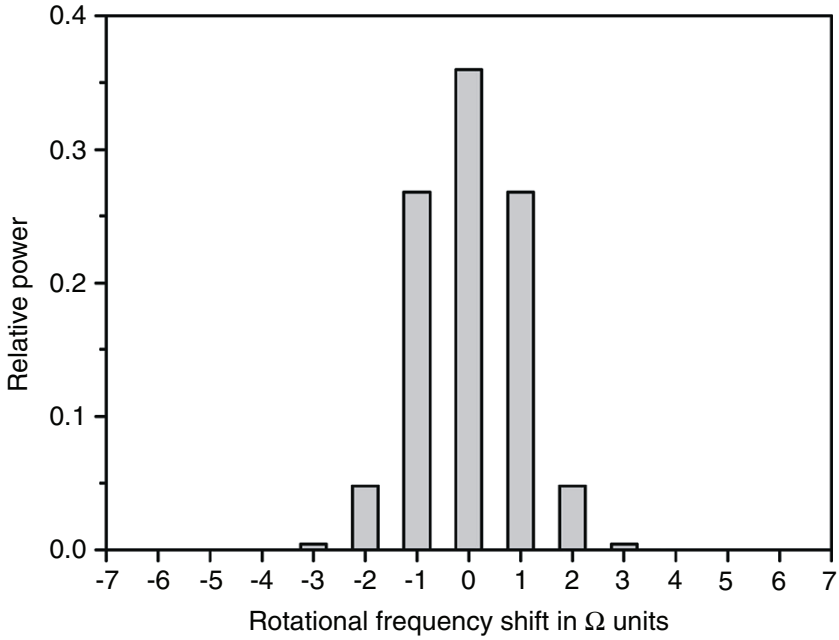

Figure 11. RDE spectrum of a rotating deflected LG_0^3 mode, corresponding to its OAM spectrum (figure 7), in Ω units, on the horizontal axis.

6. Conclusions

In two simple examples with an easily understandable geometry, we have shown how a spectrum of OAM components originates in operations of a beam's lateral displacement or tilt even for a Gaussian beam that possesses zero OAM. An off-axis beam in this case can be represented as a superposition of axial BG beams, bearing nonzero OAM values. The relative weights of these components reflect the probabilities for an individual photon to get the corresponding OAM value quantized in $\hbar$ units. The presence of the OAM components can be detected through the beam rotation, when they will attain rotational Doppler frequency shifts. Reciprocally, attributing the corresponding frequency shifts to the OAM components in the shape of BG beams, we obtain the composed beam rotation in a computer simulation. In this way, we get a confirmation of the representation of the OAM of a displaced or deflected beam through a discrete spectrum of OAM components.

For a deflected beam possessing nonzero OAM (LG mode), we found that the total OAM carried by azimuthal axial components (OAM projection) has the same absolute value as the input beam, in contrast to geometrical projection of the OAM vector. This result ensures that zero torque is acquired by the deflection element (phase wedge) and ensures zero energy variation of the beam set into rotation.

The situation may be more complicated with a simultaneous shift and tilt of a beam. The reason is that the deflected beam attains a transversal linear momentum, whose cross product with the radius vector generates an extrinsic OAM, the projection of which to the reference axis is also quantized. This additional contribution to the OAM depends on the beam orientation and therefore varies during the beam rotation around the reference axis.

We also mention the general rule for the OAM projection to an arbitrary axis. For any paraxial optical beam, created even with specific properties of noninteger topological charge

of an embedded OV [21], the OAM spectrum will reveal a discrete (generally infinite) set of components with integer per photon OAM in $\hbar$ units. The same is valid for an anisotropic OV, e.g. formed by transmission of an OV beam through a cylindrical lens. This case was analysed in [22], where the RDE effect was predicted for OV beams.

We note also the importance of the obtained results for practical application in optical communications, based on the OAM principle [23].

Acknowledgment

The authors thank Dr A Bekshaev and Professor M Padgett for valuable discussions. M Vasnetsov acknowledges grant EP/B000028/1 from the EPSRC.

References

[1] Berestetskii V B, Lifshits E M and Pitaevskii L P 1984 *Quantum Electrodynamics* 2nd edn (Oxford: Pergamon)
[2] Allen L, Beijersbergen M W, Spreeuw R J C and Woerdman J P 1992 Orbital angular momentum of light and the transformation of Laguerre–Gaussian laser modes *Phys. Rev.* A **45** 8185–9
[3] Allen L, Padgett M J and Babiker B 1999 The orbital angular momentum of light *Progress in Optics* vol 39, ed E Wolf (Amsterdam: Elsevier) pp 291–372
[4] Vasnetsov M and Staliunas K (ed) 1999 *Optical Vortices* (New York: Nova Science)
[5] Soskin M S and Vasnetsov M V 2001 Singular optics *Progress in Optics* vol 42, ed E Wolf (Amsterdam: Elsevier) pp 219–76
[6] He H, Friese M E J, Heckenberg N R and Rubinsztein-Dunlop H 1995 Direct observation of transfer of angular momentum to absorptive particles from a laser beam with a phase singularity *Phys. Rev. Lett.* **75** 826–9
[7] Courtial J, Dholakia K, Robertson D A, Allen L and Padgett M J 1998 Measurement of the rotational frequency shift imparted to a rotating light beam possessing orbital angular momentum *Phys. Rev. Lett.* **80** 3217–9
[8] Courtial J, Robertson D A, Dholakia K, Allen L and Padgett M J 1998 Rotational frequency shift of a light beam *Phys. Rev. Lett.* **81** 4828–30
[9] Di Trapani P, Berzanskis A, Minardi S, Sapone S and Chilangia W 1998 Observation of optical vortices and J_0 Bessel beams in quantum noise parametric amplification *Phys. Rev. Lett.* **81** 5133–6
[10] Mair A, Vaziri A, Weihs G and Zeilinger A 2001 Entanglement of the orbital angular momentum states of photons *Nature* **412** 313–6
[11] Leach J, Padgett M J, Barnett S M, Franke-Arnold S and Courtial J 2002 Measuring the orbital angular momentum of a single photon *Phys. Rev. Lett.* **88** 257901
[12] Vasnetsov M V, Torres J P, Petrov D V and Torner L 2003 Observation of the orbital angular momentum spectrum of a light beam *Opt. Lett.* **28** 2285–7
[13] Leach J, Courtial J, Skeldon K, Barnett S M, Franke-Arnold S and Padgett M J 2004 Interferometric methods to measure orbital and spin, or the total angular momentum of a single photon *Phys. Rev. Lett.* **92** 013601
[14] Molina-Terriza G, Torres J P and Torner L 2002 Management of the angular momentum of light: preparation of photons in multidimensional vector states of angular momentum *Phys. Rev. Lett.* **88** 013601
[15] van Enk S J and Nienhuis G 1992 Eigenfunction description of laser beams and orbital angular momentum of light *Opt. Commun.* **94** 147–58
[16] Berry M 1998 Paraxial beams of spinning light *Int. Conf. on Singular Optics* (*Proc. SPIE* vol 3487) ed M Soskin, pp 6–11
[17] O'Neil A T, MacVicar I, Allen L and Padgett M J 2002 Intrinsic and extrinsic nature of the orbital angular momentum of a light beam *Phys. Rev. Lett.* **88** 053601
[18] Abramowitz M and Stegun I (ed) 1964 *Handbook of Mathematical Functions* (Washington, DC: National Bureau of Standards)

[19] Gori F and Guattari G 1987 Bessel–Gauss beams *Opt. Commun.* **64** 491–5
[20] Orlov S and Stabinis A 2003 Free-space propagation of light field created by Bessel–Gauss and Laguerre–Gauss singular beams *Opt. Commun.* **226** 97–105
[21] Basistiy I V, Pas'ko V A, Slyusar V V, Soskin M S and Vasnetsov M V 2004 Synthesis and analysis of optical vortices with fractional topological charges *J. Opt. A: Pure Appl. Opt.* **6** S166–9
[22] Nienhuis G 1996 Doppler effect induced by rotating lenses *Opt. Commun.* **132** 8–14
[23] Gibson G, Courtial J, Padgett M, Vasnetsov M, Pas'ko V, Barnett S and Franke-Arnold S 2004 Free-space information transfer using light beams carrying orbital angular momentum *Opt. Express* **12** 5448